



Research Signpost  
37/661 (2), Fort P.O.  
Trivandrum-695 023  
Kerala, India

Recent Developments in Wear Prevention, Friction and Lubrication, 2010: 197-226  
ISBN: 978-81-308-0377-7 Editor: George K. Nikas

## 5. Tribofilms – On the crucial importance of tribologically induced surface modifications

Staffan Jacobson and Sture Hogmark

*The Tribomaterials Group at Ångström Laboratory, Uppsala University, Box 534,  
SE-751 21 Uppsala, Sweden*

**Abstract.** The interface between two solid bodies in sliding contact is an extreme environment. The local conditions typically result in substantial changes of the composition and properties of the mating surfaces. These tribologically induced surface modifications have decisive effects on the tribological performance of very different mechanical components and tools. They include topography changes (smoothing or roughening), formation of micro-cracks, phase transformations, deformation hardening, formation of oxides, formation of solid films by reactions with lubricant additives, transfer of material from the counter surface, and so on. The thickness of these layers and films range from atomic monolayers to tens of micrometres. Due to these modifications, it is *not* the original materials but the strongly modified layers that provides the wear resistance and friction level of face seals, brake pads, cutting tools, rock drills and so on.

This chapter gives an overview of this crucially important area. Due to its complexity and enormous range, this is done by presenting illustrative examples covering different materials combinations from a wide range of tribological applications.

### 1. Introduction

The interface between two solid bodies in sliding contact is an extreme environment. The local pressures, stresses and temperatures are high enough to break the bonds of even the strongest materials. Under such tribological contact the materials deform plastically and fracture on the micro scale. Atoms, molecules or larger particles are transferred between the two surfaces and to the surfaces from the environment or lubricant. The outermost layers become mixed, chemical reactions take place between the elements involved and new compounds are formed. This inferno of activities on the atomic scale and upwards often results in

the formation of films or layers of completely new materials on the surfaces, so-called tribofilms, as illustrated in Fig. 1.

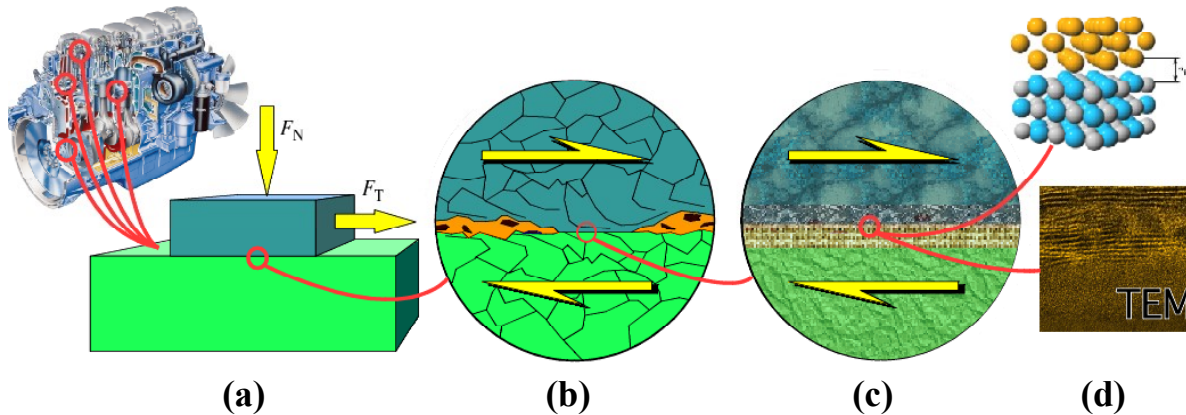


**Figure 1.** The real contact between tribological components (a) takes place on the surface asperity level, often within areas just a few  $\mu\text{m}$  wide (b). The local pressures in these micro contacts are typically several GPa. The materials may change properties down to considerable depth due to various phase transformations and deformation hardening. The outermost tribofilm (c) typically becomes nano-crystalline or amorphous and only 10-50 nm thick. The relative movement between the bodies is typically accommodated through shear deformation within this thin film, which of course results in extreme shear rates. This thin film has a decisive influence on the friction level and wear rate. It may today be studied using high resolution TEM and be predictable using atomic scale theory (d).

Hence, a significant characteristic of almost any type of dry or boundary lubricated tribological component is that the tribological properties will change dramatically during use, as a consequence of the modification of the original interface. The change may be very rapid, and thus often not even noticed, and in other cases noticeable as a slow running-in resulting in better performance of a component, a vehicle, etc. Very often the new surface materials exhibit totally different friction and wear properties compared to the original bulk materials [1–6]; the friction may be reduced or increased, the wear resistance may be better or worse.

The modifications include topography changes (smoothing or roughening), formation of micro-cracks, phase transformations, deformation hardening, formation of oxides, formation of solid films by reactions with lubricant additives, transfer of material from the counter surface, and so on. The thickness of these layers and films range from atomic monolayers (e.g. hydrogen termination of diamond surfaces) to tens of  $\mu\text{m}$  (e.g. plastic deformation of metals).

Recent developments of surface analysis techniques and high-resolution electron microscopy have revealed very thin solid films on surfaces where they previously could not be detected or analyzed. These films are often nano crystalline and partly amorphous and in the thickness range of 10–50 nm [6–11]. This chapter presents information obtained by scanning electron microscopy SEM, focused ion beam preparation (FIB) for transmission electron microscopy (TEM), scanning transmission electron microscopy (STEM), and electron energy loss spectroscopy (EELS).

Since the tribological properties of tools, wear parts, mechanical components and whole systems such as vehicles, are determined by these modified surfaces rather than by the original, they deserve attention and careful assessment. Without knowledge about how these surface layers are formed and how they modify the tribosystem, it is not possible to predict the friction and wear properties of a material in a given tribological situation. Further, the development of new materials, coatings and lubricants will be much more efficient if it is clearly understood that the surfaces will always be modified during use, and that the development should be focused on optimizing the properties after this modification.

This chapter gives an overview of this crucially important area – tribologically induced surface modifications. Due to its complexity and enormous range, it is not possible to give a full coverage. We rather try to provide insights by presenting selected illustrative examples covering very different materials combinations and a selection from a wide range of tribological applications.

## 1.1. Definition of tribofilm

Due to their complexity and multifaceted nature, these phenomena have been given many names such as transfer films, built-up layers, third bodies [12], tribolayers, tribosintered layers, selective transfer layers, self-organizing surface films [5], etc. The relations between these terms and their exact definitions have not been very clear. In the present chapter we apply the term *tribofilm* very broadly, to cover *all tribologically modified surface layers*.

## 2. Mechanisms of tribofilm formation and surface modifications

One way of organizing the tribofilm phenomena is presented in Figure 2. Here, they are classified based firstly on whether they are of the surface transformation or deposition type. For the first type of tribofilm, the outermost region of the original material is transformed due to diffusion, plastic deformation or just

frictionally heat treated. Such tribofilms have no sharp interface towards the underlying material.

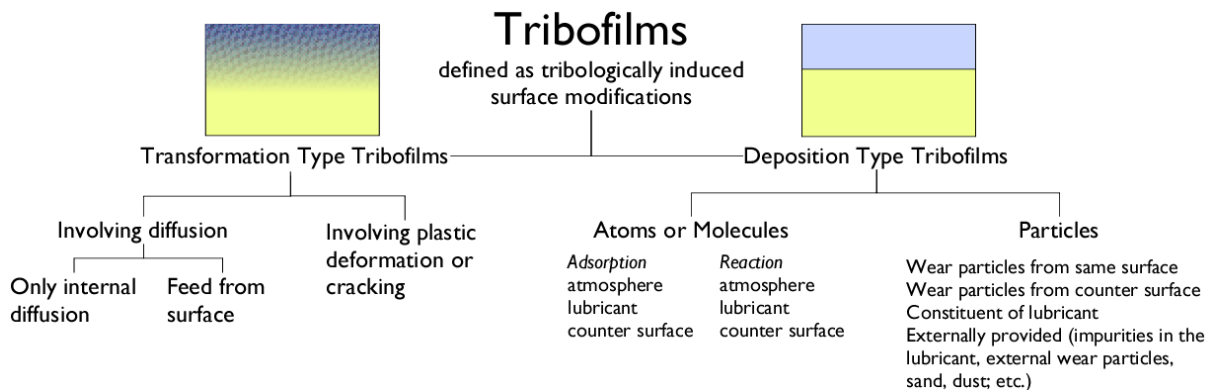


**Figure 2.** Classification of tribofilms based on whether they are formed by transformation of an existing surface layer or by formation on top of the original surface. Also combinations of these two sets of mechanisms are common.

The deposition type of tribofilms is formed on top of an existing surface by pick-up of particles, adsorption of molecules, chemical reactions, etc. These processes lead to a relatively well-defined interface, and correspondingly phenomena such as adhesion and delamination become more important here. Of course some tribofilms do not fall very clearly within one or the other type, and may involve both diffusion and pick up of particles, etc.

The *transformation type tribofilms* include two subgroups.

- (1) Films formed by transformation of the original surface involving diffusion and possibly chemical reaction and phase transformations. The diffusing atoms may originate from within the material itself or being fed from the interface, originating from the mating surface or surrounding media. This diffusion leads to local changes of composition and phase (such as second phase precipitation or dissolution), segregation, recrystallisation, grain growth, etc.
- (2) Films formed by transformation of the original surface without any material transfer or diffusion, but based on plastic deformation and crack formation. Such mechanisms lead to deformation hardening, contact fatigue, sub surface crack generation, texture formation, topography changes, grain refinement, etc. Frictional heating may cause martensitic transformations in the surface of carbon steels without diffusion across the interface.

The *deposition type tribofilms* also include two subgroups;

- (1) Films formed from individual atoms or molecules, where these are fed from the countersurface, from the lubricant or the environment and may just

adsorb on the surface, or may react chemically on the surface or with the surface atoms. Both are common mechanisms of many lubricant additives.

- (2) Films formed from larger particles that stick to or become integrated in the surface. These may be wear debris originating from the surface or the countersurface, or may be externally provided via the lubricant, etc. The particles may simply become entrapped in the interface and pressed into the surface. They may just be loosely mechanically bonded or become intimately integrated in the structure through cold-welding, sintering and similar mechanisms.

### **3. A short overview of typical tribofilms**

Tribofilms are generated in countless applications and appear in numerous forms. A presentation of some of the most common tribofilms is given below.

#### **3.1. Tribocorrosion films**

Tribocorrosion can be said to be a special family of tribofilm formation mechanisms. Here, thin films are formed by corrosive chemical reactions with components from the environment. Typically, a combination of transformation and deposition type tribofilm is generated, which may give some protection against wear, but may also be much less wear resistant than the original surface. During wear, synergistic or antagonistic effects of mechanical wear and corrosion may result in removal rates that are much lower or much higher than the sum of the individual mechanisms [13, 14].

#### **3.2. Films on oxide ceramics**

During wear of oxide ceramics, at least two types of tribofilms are often reported [2, 15-21]. One is a very thin amorphous film, the other, which is often thicker, is partly crystalline or nano crystalline and is composed mainly from compacted or sintered wear debris [22]. The small thin rolls often found on ceramics worn in the mild regime have been proposed to be formed by small removed patches of the amorphous type tribofilm, which have become curled due to residual stresses within the film [22]. Typically, oxide ceramics form deposition type tribofilms.

### 3.3. Tribofilms on low-friction coatings

Many of the popular low-friction coatings rely on the formation of a tribofilm. The detailed mechanisms and chemistry behind the formation and low-friction properties have been elegantly studied using in situ optical microscopy and Raman spectroscopy using a transparent slider [23]. By this approach, Singer et al. demonstrated that the three low-friction coatings investigated (amorphous Pb-O-Mo, DLC and annealed boron carbide) all were lubricated by thin tribofilms.

Recently several low-friction coating concepts have been developed, which all rely on formation of different tribofilms to provide the low friction [24-30]. It has been demonstrated that the low-friction performance often found for diamond in humid atmospheres is dependent on the formation and replenishment of a molecularly thin film [31–33]. So, contrary to its reputation of being a low-friction material, sliding between naked diamond surfaces *always* gives high friction. The friction forces are high enough to destroy the surfaces. It is only when the surfaces are masked by a layer of adsorbed or reacted molecules or atoms that the friction becomes low.

This layer readily forms in most atmospheres; the water content in air of normal humidity is sufficient. Adsorbed water molecules will mask the strong bonds, i.e. avoid covalent bonding between the contacting surfaces, and thus keep the friction low [34–36].

### 3.4. Tribofilms from ZDDP and other lubricant additives

Perhaps the most well-known and most studied tribofilms are those formed on ferrous metals in the presence of lubricants with the zinc dialkyldithiophosphate ZDDP additive [37–39]. This, the most successful lubricant additive in motor oils, was introduced over 60 years ago. It is still unbeaten as former of protective films on steel surfaces in combustion engines. These films are of the deposition type.

### 3.5. Transformed and transferred layers ("friction layers") on metals

In many cases metals can be considered to be smart materials; they respond to severe deformation by strengthening their structure in the surface layer. As is well known, the properties of metallic materials may alter considerably due to plastic deformation, oxidation and phase transformation. In fact, all mechanisms known for strengthening of bulk crystalline materials [40] can be activated locally in the surface layer during tribological contact. This includes both transformation type tribofilm formation in the form of deformation hardening (dislocation strengthening), grain refinement (Hall-Petch strengthening, also due to

deformation), hard phase generation (e.g. martensitic transformations in steel), solute strengthening (alloying by diffusion), and deposition type tribofilm formation in the form of particle strengthening (e.g. oxide particle intermixing), composite strengthening (pick-up of counter material or wear particles), etc.

The success of metals as tribological materials is partly explained by the fact that these changes often act to improve the wear resistance [41, 42]. Selected examples of hardness and structure changes in structural steels subjected to severe abrasion have been presented in [43] and [44].

## **4. Illustrative examples**

### **4.1. A unique tribofilm of the transformation type accounts for the low-friction behavior of Stellites**

Stellites – a family of Co based chromium alloyed metals – are well known for their good low-friction and anti-galling behavior in heavily loaded, unlubricated contacts. These properties make Stellites very popular as hardfacing materials for components in demanding tribological applications such as heavy duty valves, turbines, spindles, etc. [45]. In dry contacts they typically generate friction coefficients of the order of 0.20–0.25, and show a very good resistance against material pick-up and galling.

This performance has often been attributed to beneficial thermal and chemical/corrosive properties. However, with the aid of modern analytical techniques, Persson has recently revealed the mechanism behind this behavior [45]. Self-mated Stellite 21 surfaces exposed to dry reciprocating sliding, exhibited a phase transformation from bcc to hcp down to a depth of about 100  $\mu\text{m}$ . Also, a substantial hardness increase was detected in this layer. In the most superficial  $\approx 10$  nm layer, the hcp basal planes were further more lined up parallel to the surface (see Fig. 3a). The latter process offers easy dislocation glide parallel to the sliding direction. In this way, the ideal situation of a hard, load bearing layer (i.e. minimized real contact area) with an easily sheared surface film is created. The whole procedure is repeated as soon as the superficial layer is worn off. The fcc to hcp transformation occurred also at lower contact pressures, but no alignment of the basal planes along the sliding direction was observed (cp. Fig. 3b), and the friction coefficient was higher around 0.4.

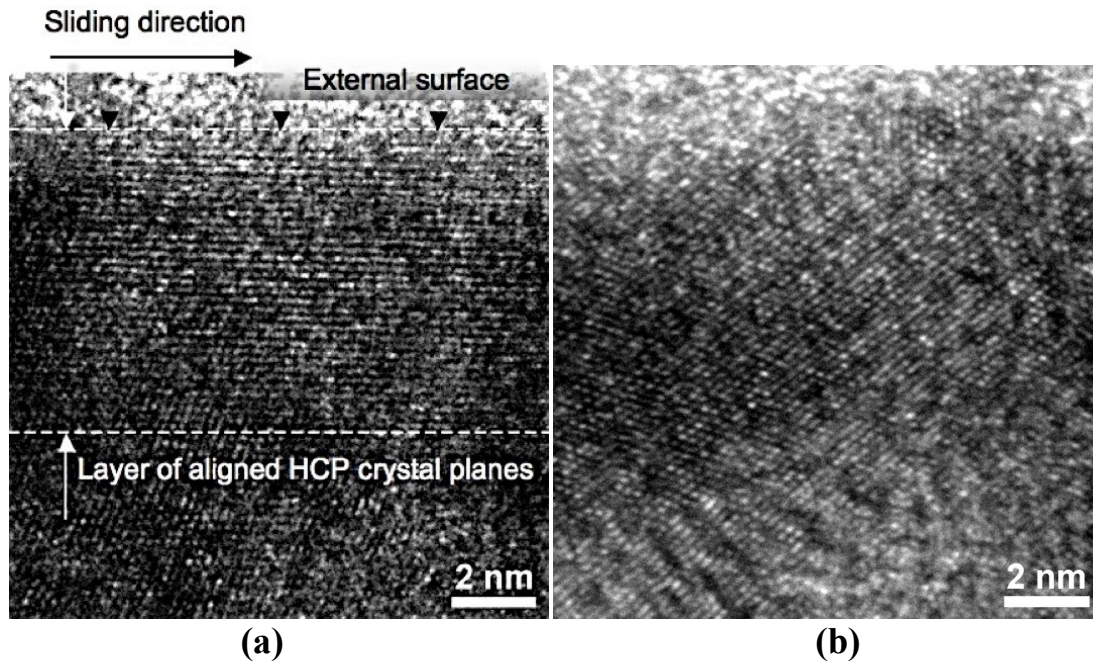


**Figure 3.** High-resolution TEM micrographs of cross-sectioned surface layers of Stellite 21. (a) Surface deformed by heavily loaded dry sliding. Notice the key to the low-friction behavior – the formation of the 10 nm thin, easily sheared top layer within which the hcp basal planes have become oriented parallel to the worn surface. (b) Ground surface. As in (a), the outermost atomic layers have completely transformed from fcc to hcp. However, unlike the case of the heavily loaded sliding contact no preferential orientation can be observed [45]. (Stellite 21: in wt% 27 Cr, 0.25 C, 5.5 Mo, 1.5 Si, 1.0 Mn, 2.5 Ni, < 3 Fe, bal. Co.)

## Conclusion

Three separate transformation type tribofilm mechanisms explains the unique tribological behavior of Stellite. Firstly, the stress induced deformation hardening and secondly phase transformation of the Co matrix from the fcc structure of the bulk to hcp in the surface layer. Thirdly, in the outermost layers the shear stress acts to align the hcp structure with its easy-to-shear basal planes parallel to the sliding interface.

This model as illustrated in Fig. 4 [45, 9] explains the intrinsic low-friction and anti-galling properties of the Stellites in heavily loaded sliding contacts. The oxide layer does not play any major role in the mechanisms described, indicating that Stellites would function equally well in water, vacuum and other oxygen free environments.

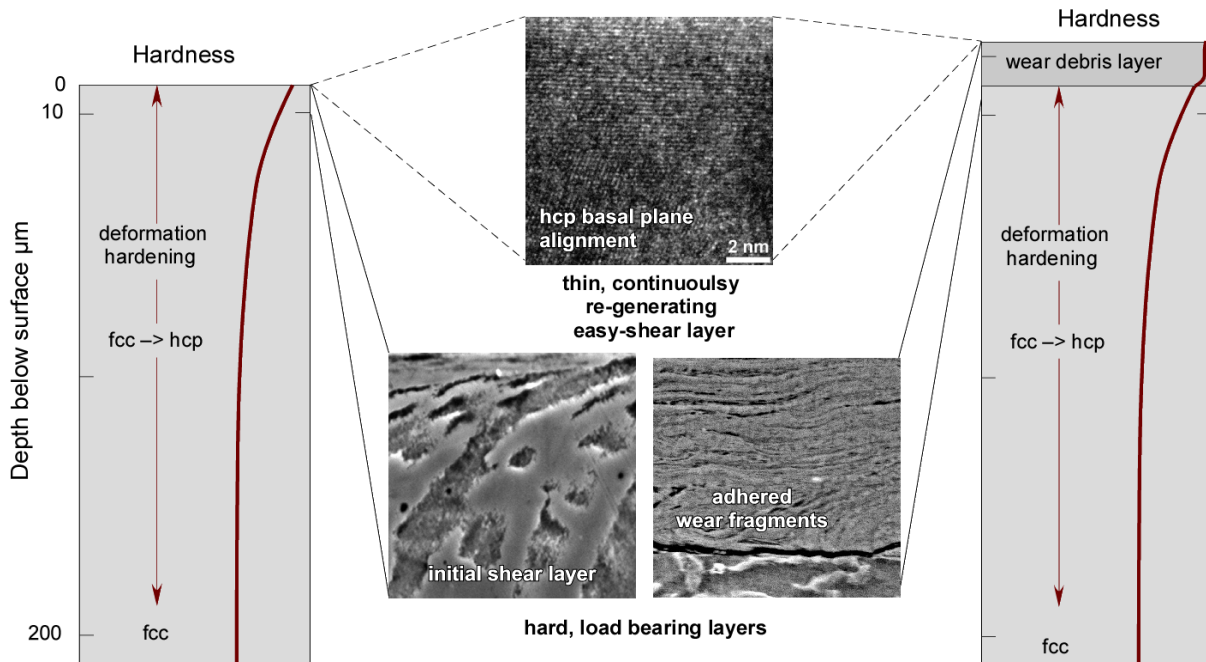


**Figure 4.** Schematic view of the self-generating low-friction system of Stellites typical of highly loaded sliding contacts. The hardness is increased down to substantial depth and the ultra-thin (just a few atomic layers) easily sheared aligned hcp layer continuously regenerates at the surface (left graph). The easy-shear layer forms equally well on surfaces involving a layer of accumulated wear debris (right graph) [45, 9].

#### 4.2. Galling on forming tools is caused by problematic tribofilm formation

Plastic forming of austenitic stainless steel has proven to be one of the most demanding tooling operations. The reason is the extreme tendency of this type of work material to adhere to the tool. Lumps of steel adhered to the tool surface will cause damage to the next products to be formed. This process of adhesion and subsequent damage is usually named galling.

It is well documented that the primary reason behind most of the galling problems in industrial forming is related to a rough tool topography [46,47]. For sufficiently smooth tools, the general belief has been that adhesion occurs when any oxide or lubricant is removed from the interface such that the work and tool materials are making metallic contact on the atomic level.

However, recent studies in a Load Scanner test [48] revealed an oxidic interlayer between adhered stainless steel and the tool [8]. It was even shown that, on some areas of the sliding track, no *metal* from the stainless steel work piece had

become transferred but the tool surface was covered with *oxide* transferred from the stainless steel.

One conclusion is that the adhesion of the stainless steel oxide (mainly CrO) to the tool steel is at least as strong as the adhesion to its parent steel, another is that metallic contact is not an absolute prerequisite to adhesion and galling.

Previously unpublished results presented in figures 5-7 reveal that there is an oxidic interlayer between the tool and transferred work material also for industrial tools that have been used to form a large number of austenitic stainless steel sheet components.

The tool is made of a powder, metallurgical, cold-working steel with the nominal composition (wt%) of 9V, 4.5W, 5 Cr and 4 Mo. It was hardened and tempered to about 60 HRC. The stainless steel is of the AISI 304 type (18.5 Cr and 10 Ni). Areas where stainless steel had adhered were identified in the SEM, and specimens for TEM-studies were prepared using a focused ion beam (FIB) instrument, see Fig. 5.

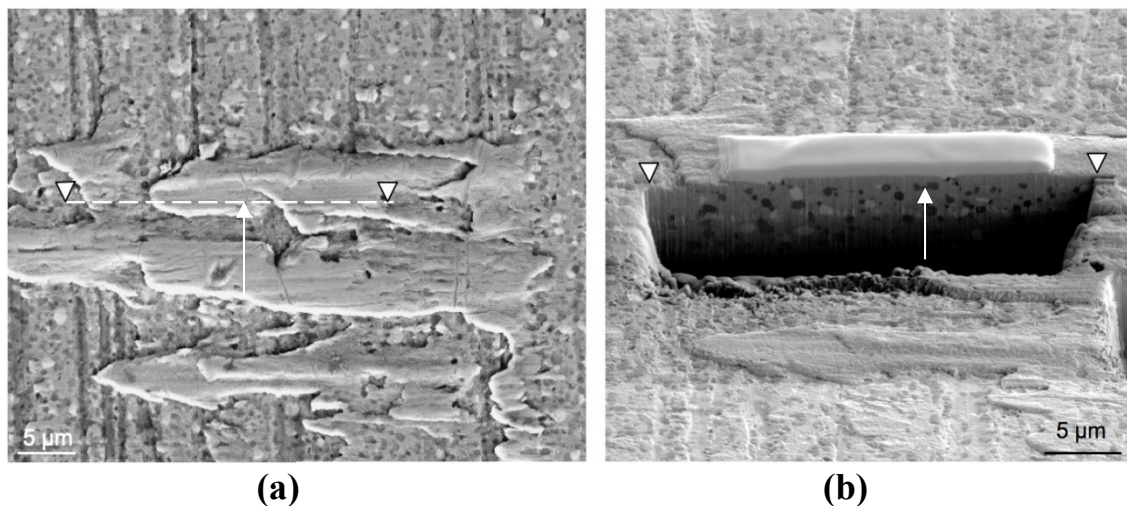


**Figure 5.** (a) Appearance of PM tool steel surface where some patches of austenitic stainless steel have adhered during sheet forming. The direction of sheet sliding during forming was from left to right. (b) A crater in the tool surface formed by the FIB along the dashed line in (a). A similar crater was subsequently formed slightly above the dashed line to leave a thin disk of tool steel with adhered stainless steel as the TEM specimen. Thus, this specimen is perpendicular to the tool surface and contains the interface between tool and work material. The arrows in (a) and (b) indicate the location of the TEM pictures in figures 6 and 7.

TEM studies (figures 6 and 7) reveal an oxidic interlayer (20-60 nm thick) between the tool steel and the adhered austenitic stainless steel. It is made up of a combination of Fe, Cr and V oxides, and contains carbon from the forming oil.

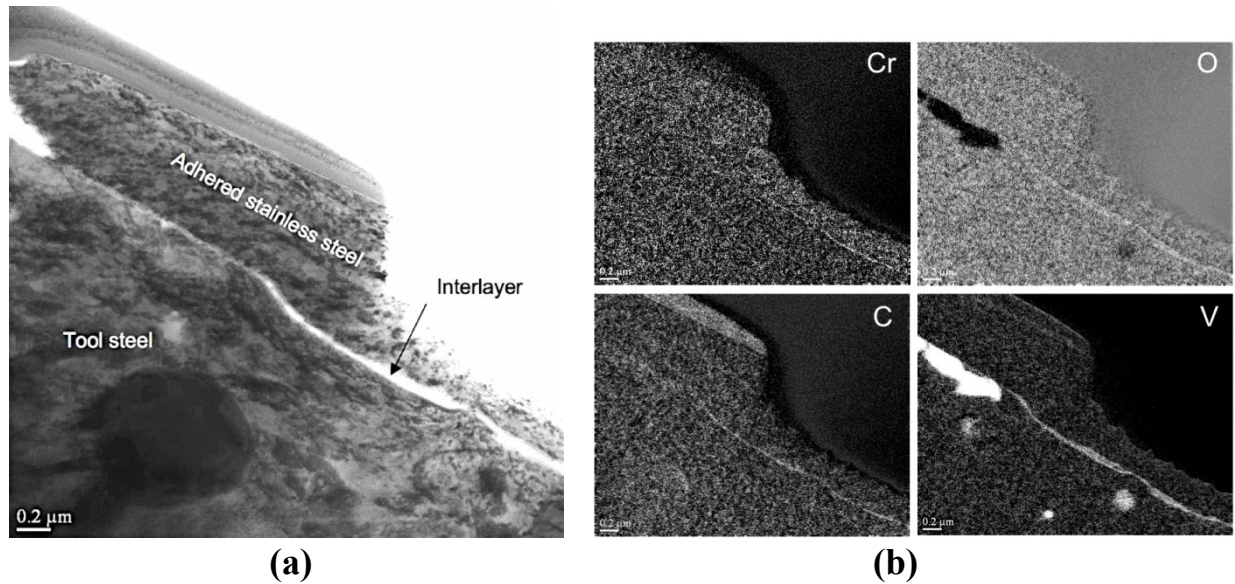


**Figure 6.** (a) TEM cross-section micrograph showing austenitic stainless steel adhering to the tool steel. The light contrast of the interlayer between the tool steel and the stainless steel is due to its amorphous structure in combination with its high concentration of light elements (mainly O and C). (b) Elemental mapping using electron energy loss spectroscopy (EELS) of the same area as in (a). Note the slightly reduced magnification.

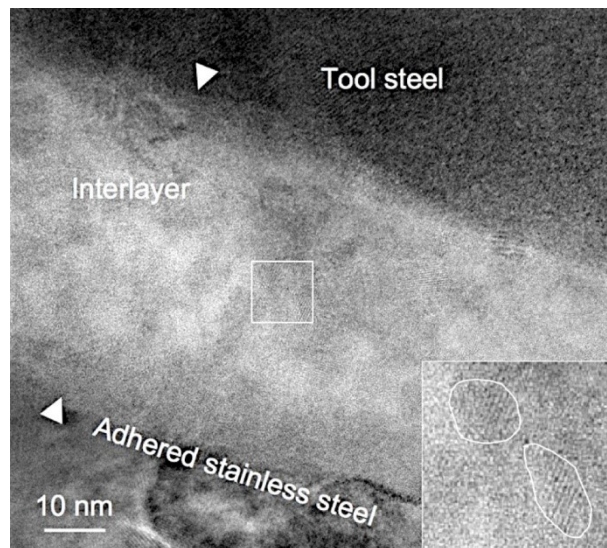


**Figure 7.** High resolution TEM of the interlayer between adhered stainless steel and tool steel shown in Fig. 6. Note that the structure is in the form of an amorphous matrix with nanometer-sized crystallites (encircled in the magnified insert).

## Conclusion

Formation of a tribofilm of the deposition type is responsible for the galling phenomenon. It is made up of two layers; one thin very fine grained or amorphous oxide layer next to the tool surface followed by a heavily deformed fine grained layer of stainless steel. The strength of the thin oxide layer is obviously higher than the cohesive strength of the austenitic stainless steel. Usually, the strong galling tendency of austenitic stainless steels is attributed to their combination of strong ability for deformation hardening, their thin natural oxide layer (of the order of 5-10 nm) and their relatively low heat conductivity (about half of that of carbon steel). However, we have shown that the formation of an extremely strong and adhesive oxidic tribofilm may be the primary explanation. This oxide obviously acts as a very strong weld or glue between the tool steel and the stainless steel. It is composed of elements (fragments) from both tool and work material (Fe, V, Cr) and from reactions with the environment (O and C).

### 4.3. Tribofilms protect metal cutting tools

Machining of steels can be very demanding for the cutting tool. This is illustrated by the wear mechanisms activated when cutting a H14 type of hot working tool steel with a cemented carbide (CC) tool [44, 7]. The SEM and FIB technique was used to make cross-sections through the rake face of a cutting insert. After having identified an area where some work material (tool steel) had adhered, a TEM specimen was produced by ion beam milling, see Fig. 8. After cutting loose the TEM specimen and preparing it by further ion beam thinning, STEM imaging was performed – see figures 9 to 11. In this mode, EDS was used to determine the elemental composition of interesting features around the tool steel – CC tool interface, cp. Fig. 10. The structure of the interface was best studied by conventional TEM. The WC grains, Co-binder and adhered steel could be resolved – see Fig. 11. It is revealed that the wear of CC occurs by a mechanism involving formation of a deposition type of tribofilm. (In the metal cutting community usually denoted built-up layer.) The film is continually deposited and removed by plastic shear. Although being formed by tool steel – normally a much weaker material than the CC – the shearing tribofilm is strong enough to gradually remove the Co-binder of the CC material. Subsequently, the hard WC grains also become fragmented and removed as part of the shearing tribofilm – see Fig. 10. The strength of the tribofilm is primarily due to its extremely fine grain size, cp. Fig. 11.

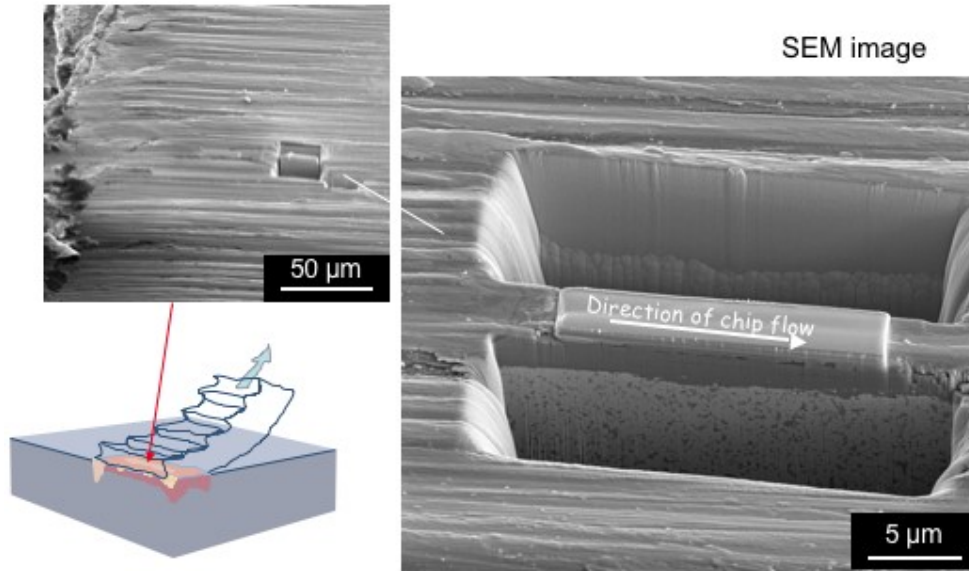


**Figure 8.** SEM micrographs of the rake face of a cemented carbide CC cutting tool showing (in two magnifications) where a cross-section is made using the FIB-SEM. The tool has been cutting in carbon steel, some of which is adhered to the rake face.

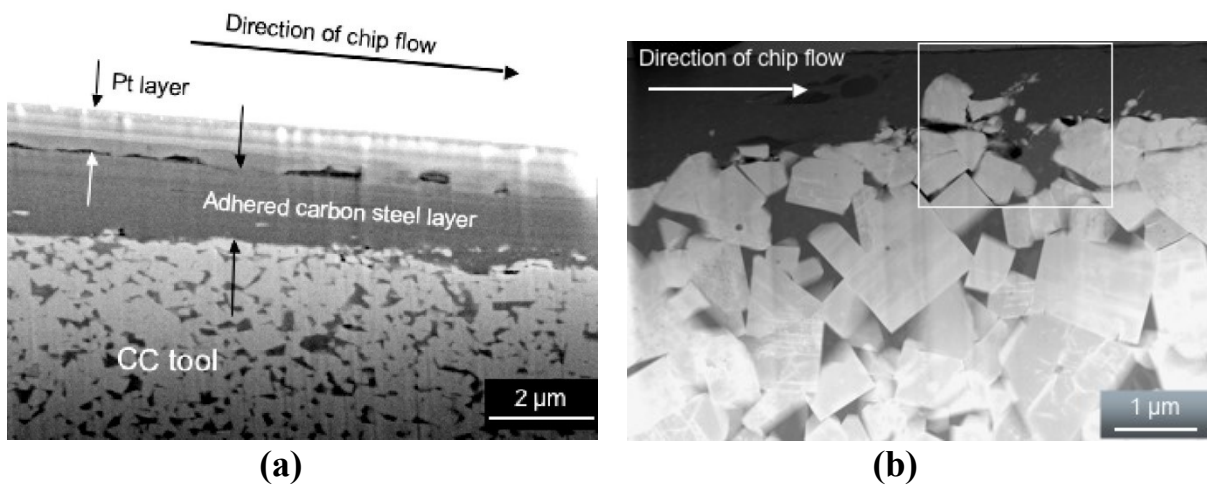


**Figure 9.** Close-up of the cross-section in Fig. 8. (a) The top layer of Pt is deposited to protect the external surface of the tribofilm (mainly consisting of adhered steel) during the preparation. SEM (b) STEM micrograph of the tribofilm/CC interface region. (CC = WC grains in a matrix of Co.) The light particles are WC grains of the CC, the intermediate grey material is the Co binder, and the dark grey layer is the transferred carbon steel. The area for further TEM studies (Fig. 10) is indicated by the white rectangle.

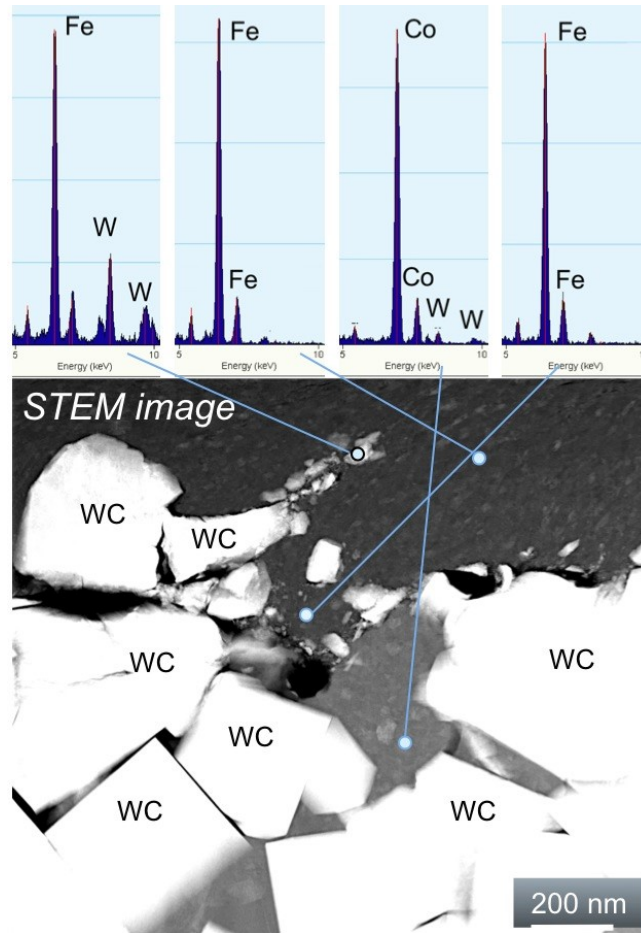


**Figure 10.** STEM micrograph and selected EDS spectra of the tribofilm/CC interface region. Note the entrainment of steel into the cemented carbide structure, the fragmentation of the outermost WC grains and the inclusion of the small fragments into the shearing adhered steel layer, see also Fig. 11.

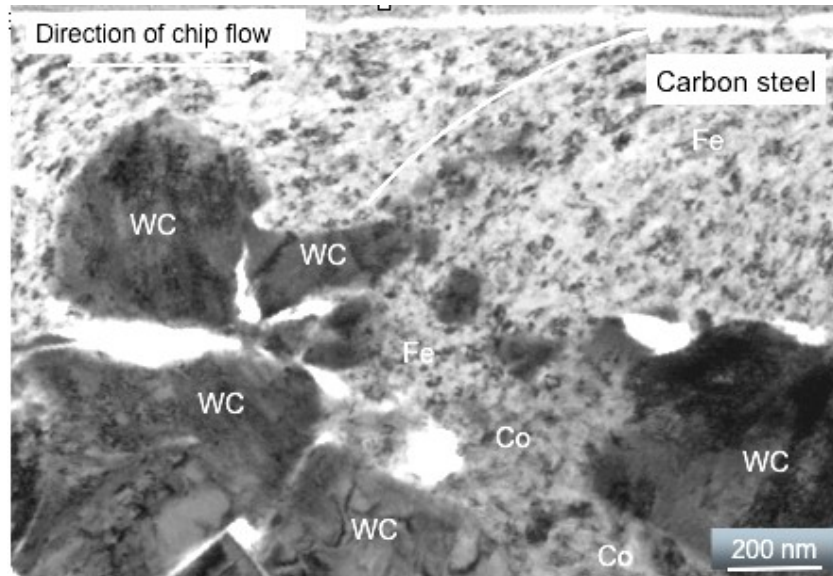


**Figure 11.** TEM micrograph revealing the crystallographic structure of the interface region between the adhered work material (carbon steel) and the CC tool material. White areas represent voids in the CC material formed by the deformation involved in the removal of the solid WC grains. (Same area as in Fig. 10.)

Some metallic materials such as aluminium and titanium alloys and austenitic stainless steel are generally regarded as being difficult to machine since they easily form strong built up layers. For the stainless steels, this has led to the development of so called free-machining steels, i.e. grades that have been alloyed to contain a small proportion of, for instance, inclusions of manganese sulphide (MnS). (Formed from Mn and S added to the steel.) During cutting, a thin tribofilm of MnS will adhere to the tool and act as a solid lubricant, and protect the tool from wear. However, free-machining grades have a lower corrosion resistance and slightly reduced ductility as compared to their non-free machining equivalents because of the presence of these non-metallic inclusions.

## Conclusion

Tribofilms associated with metal cutting are usually of the deposition type. They are generally believed to protect the cutting tool from wear even if they contribute to the wear mechanisms. However, if they grow in thickness to form built up edges, they may cause chipping of the cutting edge and also degrade the surface roughness of the cut product.

#### 4.4. Tribofilm formation on self-mated ceramic face seals – optimum recycling of wear debris

Face seals are used in many harsh applications, for instance in submersible pumps where an electric motor has to be sealed from the outside media. If this media contains hard particles such as sand, it is not possible to use rubber seals. Instead, seals in the form of two disks with central holes are used (see insets in figures 12 and 13). The seals are pressed against each other face to face and have to be flat and smooth to effectively prevent e.g. water to leak from the high-pressure side to the low-pressure side during the rotation [2, 20, 21, 49]. Typical materials in such components are cemented carbide (CC), alumina ( $\text{Al}_2\text{O}_3$ ) and silicon carbide (SiC).

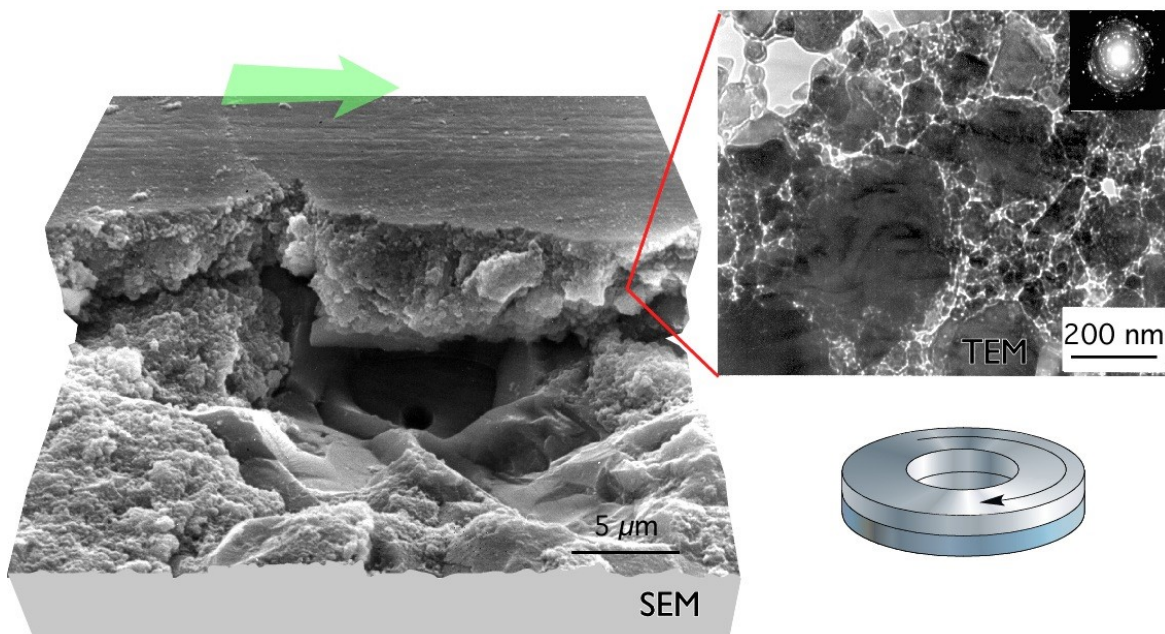


**Figure 12.** Tribofilm formation on a ceramic (alumina) face seal. The wear debris is to a high degree retained in the closed contact between the two plane seals, which give a high probability to become recycled as a wear protective tribofilm. The TEM micrograph reveals a tribosintered deposition type of film consisting of relatively loosely bonded alumina fragments [2, 20, 21]. The arrow indicates the sliding direction of the counter body.

Figure 12 shows a detail of the surface of an alumina face seal. During use, a 5  $\mu\text{m}$  thick film of alumina debris has formed. A small part of this almost fully covering film is present in the upper part of the figure. Note that the top surface of the tribofilm is much smoother than the worn bulk surface beneath (lower part of

the figure). This reveals a positive effect from this type of film formation (less leakage). Another obvious benefit is wear protection.

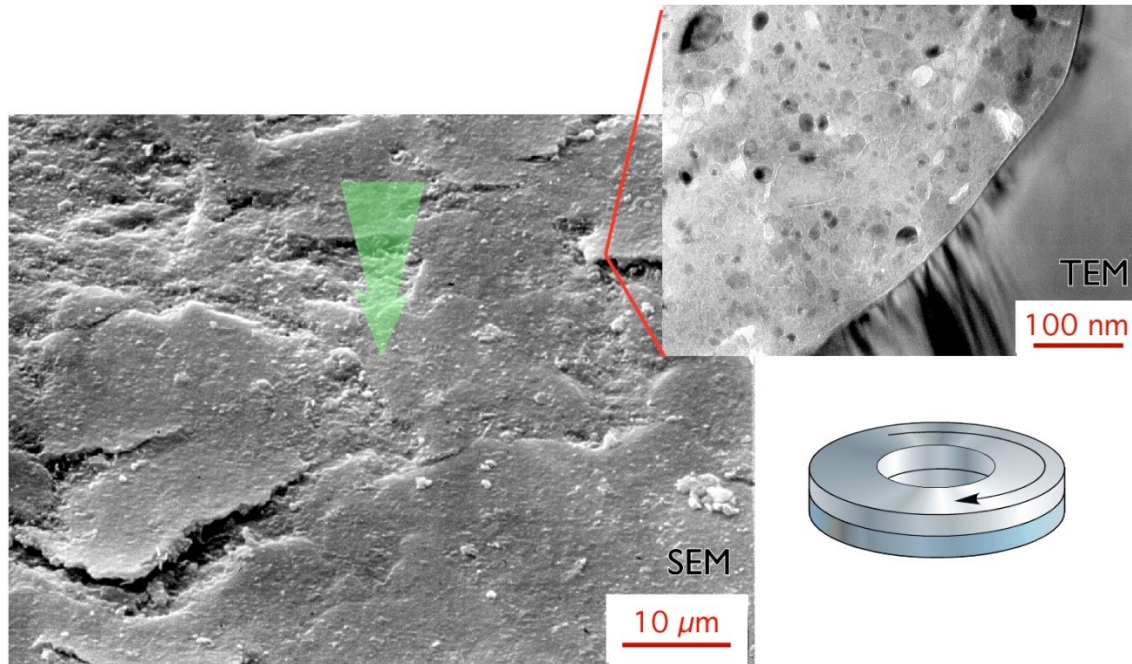


**Figure 13.** Tribofilm formation on a ceramic (SiC) face seal exposed to sliding in dry air. SiC against SiC results in a film of SiC nano-crystals embedded in a dense SiO<sub>2</sub> matrix, firmly bonded to the underlying unworn SiC grain [2, 20, 21]. Left SEM picture of the top surface, showing an almost entirely covering tribofilm. Top right TEM picture showing the dense structure of the tribofilm and the intimate bond towards the SiC grain. The arrow indicates the sliding direction of the counter body.

Figure 13 shows a similar set of micrographs representing a face seal of SiC that has been running under conditions identical to those of the alumina seal. Also here a deposition type tribofilm is formed. It is smooth and covers almost the entire nominal contact area. Compared to that of alumina, it is thinner and denser. The TEM micrograph shows the interface between the tribofilm (upper left) and the SiC material (lower right). The interface is very sharp. The structure is revealed to contain nano sized SiC particles (dark grains in the image) embedded in a matrix of amorphous SiO<sub>2</sub>. This means that the SiC debris have gradually oxidized during the tribosintering process [20,21]. The positive effect of tribofilm formation is here threefold; smoothening (reduced leakage), wear protection and friction reduction. Typically, the dry friction level associated with this SiO<sub>2</sub>-based tribofilm is of the order of 0.2 to 0.3.

## Conclusion

The tribofilms from these two examples of self-mated ceramic materials are of the deposition type. During running-in, they effectively improve the function of the seals by smoothening the contact surfaces, and they also protect the surface from further wear. For the SiC seals the films also contribute to a significantly reduced friction, which means a reduced energy loss through the seal.

### **4.5. Tribofilm formation on drive elements of micromotors provides the necessary grip**

Ultrasonic motors are often very attractive in applications where miniature size, high speed, good precision and low power consumption are essential features. Traditional motor technology uses gearboxes or lead screws and nuts to accomplish linear movement. Such miniaturized systems are complicated to manufacture and assemble, while piezoelectric motors based on direct friction drive systems are well adapted to miniaturization.

The principle of one such ultrasonic piezoelectric motor is shown by the insert in Fig. 14. When appropriate drive signals are applied to the piezoelectric elements, they oscillate in such a way that the attached cylindrical drive pads describe an elliptical motion. To achieve the linear motion, the drive pads transfer the movement to the drive rail by gripping and pushing it forward during each half cycle. The rail is pushed approximately 1  $\mu\text{m}$  per cycle, at a frequency of 96 kHz. The total stroke is in this case 6 mm. The pads and rail consist of alumina, selected based on its relatively low wear rate and relatively high coefficient of friction.

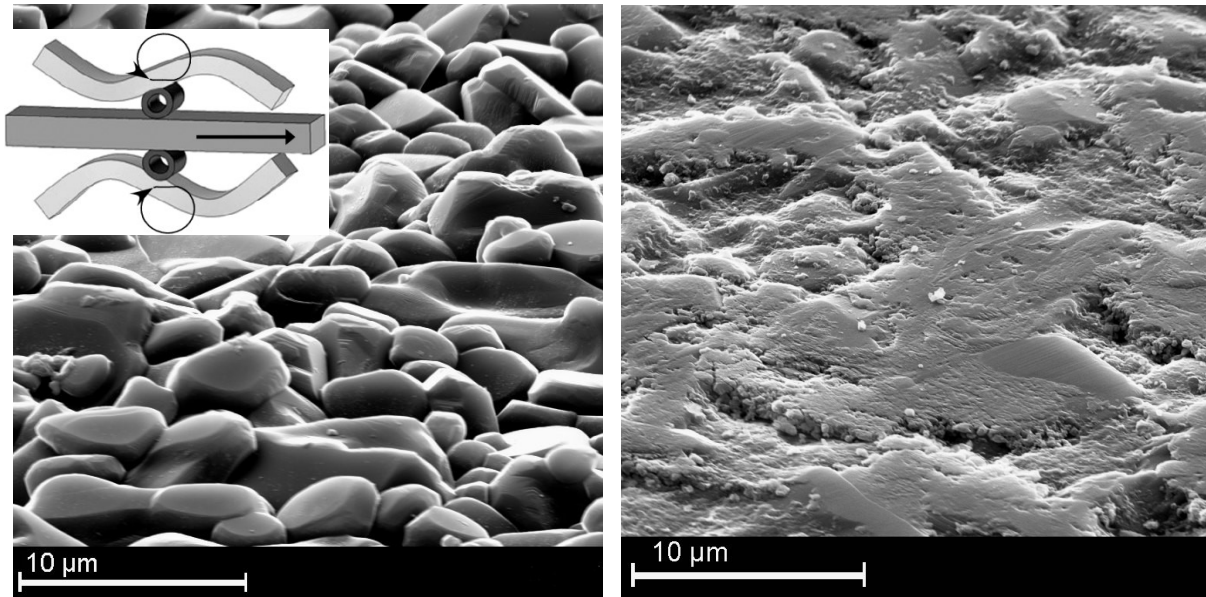


**Figure 14.** Appearance of the alumina drive rail from the friction drive system of a linear piezoelectric micromotor. Left: the as sintered surface before use. Right: after about 350,000 strokes of the rail. Inserted: schematic of the drive system consisting of a driven central alumina rail and two piezoelectric vibrating beams that transfer their vibrating movement to a linear translation of the rail via two hollow alumina drive pads [16].

The as sintered surfaces initially wear very rapidly, resulting in flattening of the most protruding alumina grains, and correspondingly high production of wear debris. This debris rapidly fills the cavities between the grains and is efficiently squeezed and worked to form a dense tribofilm – see Fig. 15. The film becomes mostly amorphous and partly nano crystalline, and develops a very intimate bond to the unworn grains [15, 16]. Unprotected edges of the film will easily become worn off again, so even if the initially rapid wear rate of the ceramic soon levels off, there will be some circulation of debris that first form tribofilms, then fracture again into debris, participate in the new film formation, and so on.

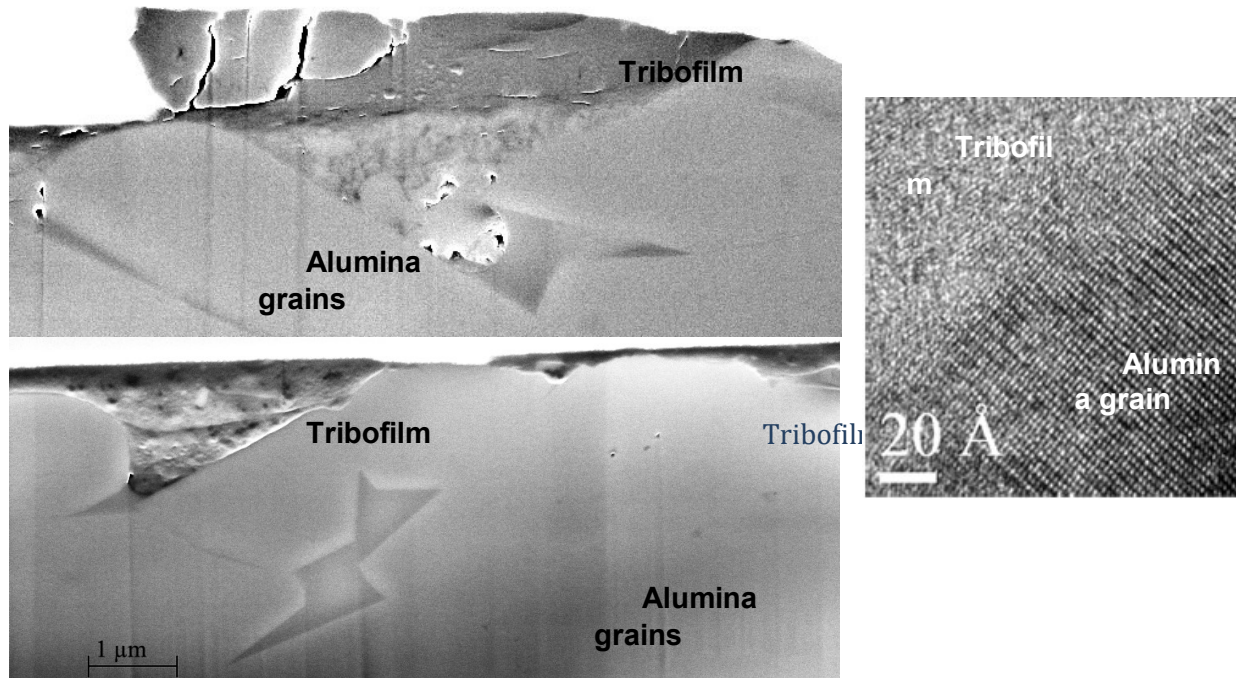


**Figure 15.** Cross sections of a drive rail after about 200,000 strokes. A relatively thick tribofilm consisting of sintered or compacted wear debris fills out the cavities between the unworn alumina grains. A thinner tribofilm partly covers the top parts of the alumina grains that have become worn flat [16]. Top: tribofilm with several cracks indicating that this unprotected part of the tribofilm is repeatedly worn and rebuilt (SEM). Bottom: tribofilm stabilized by the protecting surrounding alumina grains (left) and thin film partly covering worn area of the alumina grains (right) (SEM). Right: high resolution TEM illustrating the virtually perfect bond between the mainly amorphous tribofilm filling out a cavity and the neighboring crystalline alumina grain (TEM).

## Conclusion

In this case the tribofilm gives some wear protection, and furthermore it provides a higher friction coefficient than the original surface. The high friction coefficient is necessary for the proper operation of the friction driven motor [15, 16].

## 4.6. Complex tribofilms bring the car to a halt

The disc against pad interface of automotive brakes is a fascinating world of intense tribological activity. Surfaces are wearing and reforming, local contact areas are born, grow, mature and die while legions of micron sized and nanometer

sized particles rush along the constantly reshaping maze formed between the irregular pad and relatively flat disc – see Fig. 16.

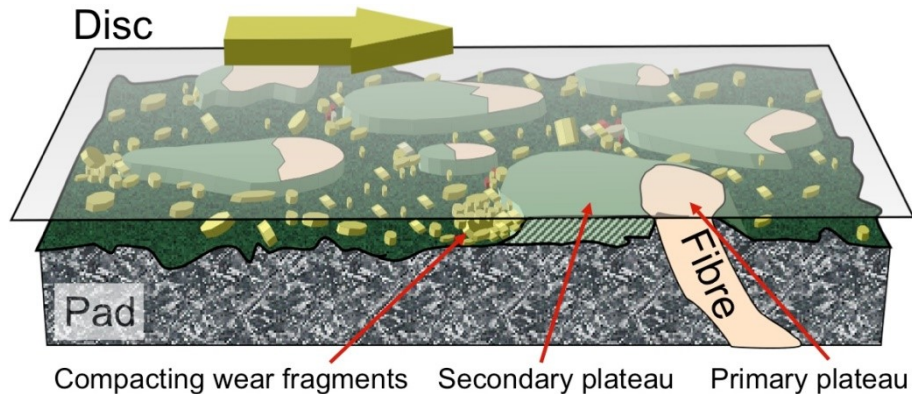


**Figure 16.** Schematic of the contact situation between brake disc and pad according to the plateau model. The disc sliding direction is from left to right. Protruding hard phase constituents, i.e. primary plateaus of the pad are white, compacted debris in the form of secondary plateaus are grey. A constant flow of wear debris in the gap between pad and disc wears the lower regions of the pad through three body abrasion and supply the secondary plateaus with new material. Occasionally secondary plateaus break down, releasing heavily deformed particles back to the flow of wear debris [50].

The brake must deliver a relatively high and totally reliable coefficient of friction, regardless of speed, temperature, pressure, presence of water, contaminants, etc. It must deliver this friction without too much wear, without seizure, while causing minimum vibrations and squeal [51].

Primarily based on an unconventional study involving direct observation of the contact interface through a glass disc, Eriksson et al. [52] could describe the buildup and breakdown of the contact plateaus formed in the gap between disc and pad. Wear debris was observed compacting against hard phases, e.g. steel fibers and quartz particles, of the brake pad forming flakes of agglomerated particles. Based on this and a series of other studies, a model for the formation of the contact interface was presented [50, 53]. The mechanism proposed to cause the formation and growth of contact plateaus is described by the plateau model, illustrated in Fig. 16. It involves a pad surface in sliding contact against a disc, where protruding hard phases, called the primary plateaus, initially take up the major part the load and shear stress in the contact. Against these primary plateaus wear debris is compacted, forming secondary plateaus. The lower regions surrounding the plateaus wears by three body abrasion at the same wear rate as the plateaus.

A secondary plateau (Fig. 17) was studied more closely by using a SEM equipped with a field emission gun (FEG) electron source. It was shown that the

outermost surface of the secondary plateau has been sintered, forming a hard amorphous or nanocrystalline layer [50]. Further down in the plateau the grains get coarser and less compacted. A diffuse structure was spotted at or just below the surface, with particle sizes down to 5-10 nm, cp. Fig. 18. When looking at the detached secondary plateau from below, considerably larger grains were found, with a typical size range of 0.1 to 1  $\mu\text{m}$ . It was concluded that the secondary plateau of the standard brake pad of a Volvo passenger car mainly consisted of iron oxide with the iron to oxygen ratio around 4/5. Small amounts of sulphur and copper were found scattered over the surface except on the primary plateaus. Surprisingly, despite the abundant supply of carbon-containing materials, almost no carbon was detected on the contact plateaus.

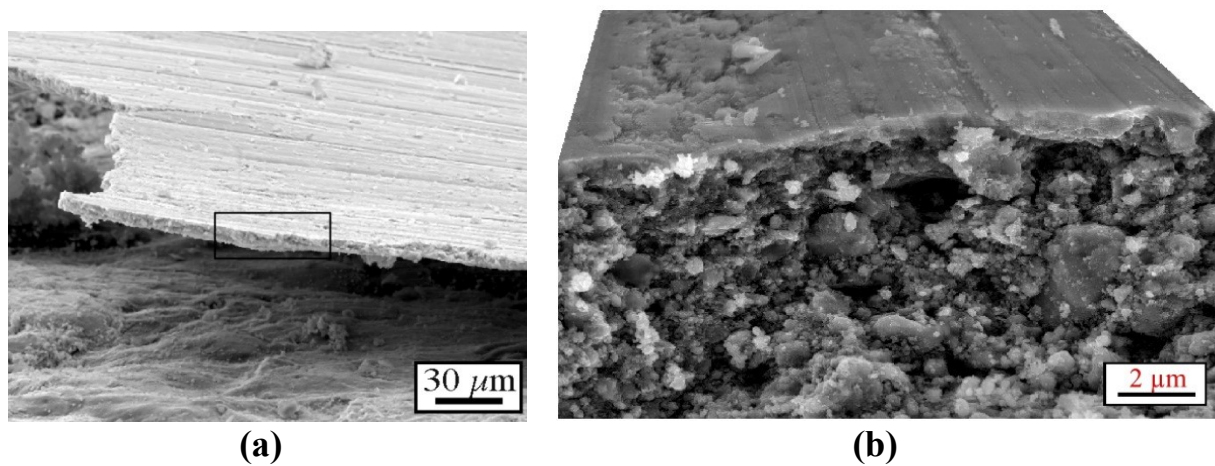


**Figure 17.** Partly detached secondary plateau. (a) Overview showing its thin flake like shape. (b) Detail showing the structure of relatively porous partly tribosintered debris topped by a very dense mostly amorphous top layer.

Obviously, it takes several consecutive steps to form the complex and dynamically responding tribofilm on the pads. A superficial very thin film covers both the primary and secondary plateaus. It is the flow properties of this film that account for the friction resistance.

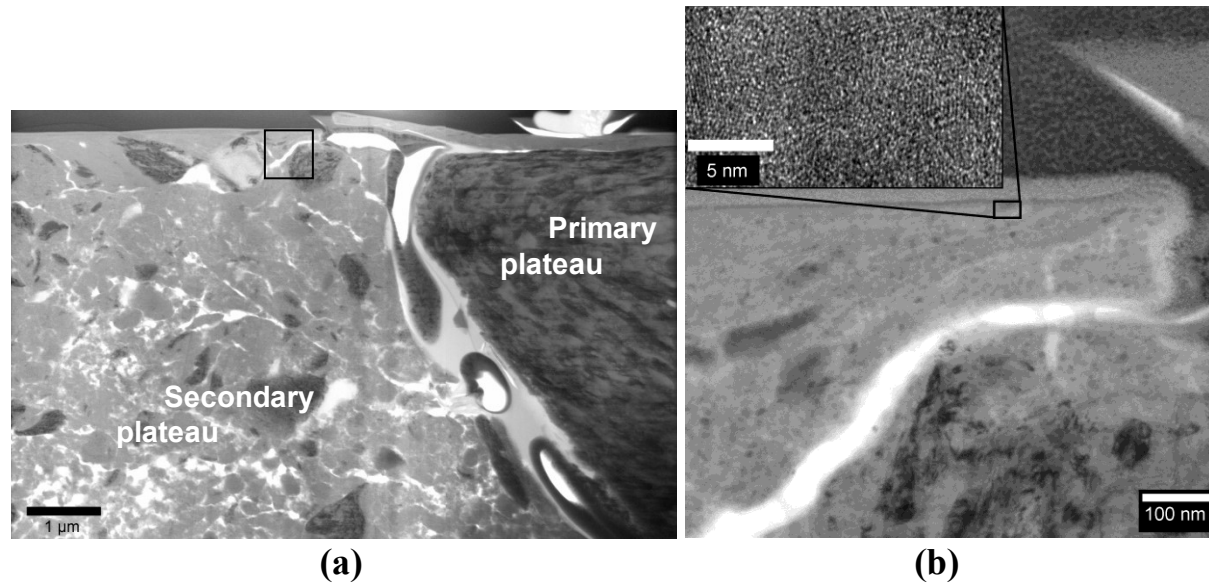


**Figure 18.** Cross-section of the transition area from secondary plateau (compacted debris on the left) to a primary plateau based on a steel fiber (right). The disc has been sliding against the upper surface from left to right. (TEM in bright field mode.) (a) Both primary and secondary parts of the contact plateau are covered by a thin tribofilm (medium grey, dense but broken above the crack separating the two parts). A gradient in degree of compaction in the secondary plateau is very clear, with the most loosely compacted debris at the bottom. The area shown in (b) is indicated by a black frame. (b) Detail indicating a flow in the sintered iron oxide following the shape of an iron particle. Inset: high-resolution image showing the dense amorphous character of the most superficial sintered material.

The superficial film is distinguished by being:

- nanocrystalline, with a typical grain size of around 5 nm;
- fully dense;
- very thin (we have typically noted 50–200 nm, Österle reported 100 nm [10]);
- very hard compared to the underlying secondary plateau and the medium hardness of the pad, and harder than the disc [50], and
- forming on both the primary and secondary plateaus, and
- having a composition dominated by iron oxides (Österle has in some cases noted magnetite to be the prominent phase of iron oxide [10].)

## Conclusion

The tribofilms formed on automotive brake pads are of a complex deposition type. The highly dynamic formation process involves compaction of wear debris

and tribosintering forming a very thin (50–200 nm) glassy or nanocrystalline top layer. It is this vanishingly thin top layer of the tribofilm that accommodates the relative movement and provides the required stable coefficient of friction  $\mu \approx 0.4\text{--}0.5$ . Despite the complex composition of a typical organic pad, including some 30 ingredients, this active top layer is dominated by nanocrystalline iron oxide.

#### 4.7. The dramatic surface modification of rock drill buttons

One of the most demanding tribological applications is percussive rock drilling. The best materials to resist this situation of high impact against rock materials are coarse-grained WC/Co cemented carbides (CC). For a long time, these materials were primarily optimized to resist impact and abrasive wear. However, in his Ph.D. thesis, Ulrik Beste showed that the surface of the CC drill bits typically transforms into a totally different material before being removed [11, 35, 54, 56].

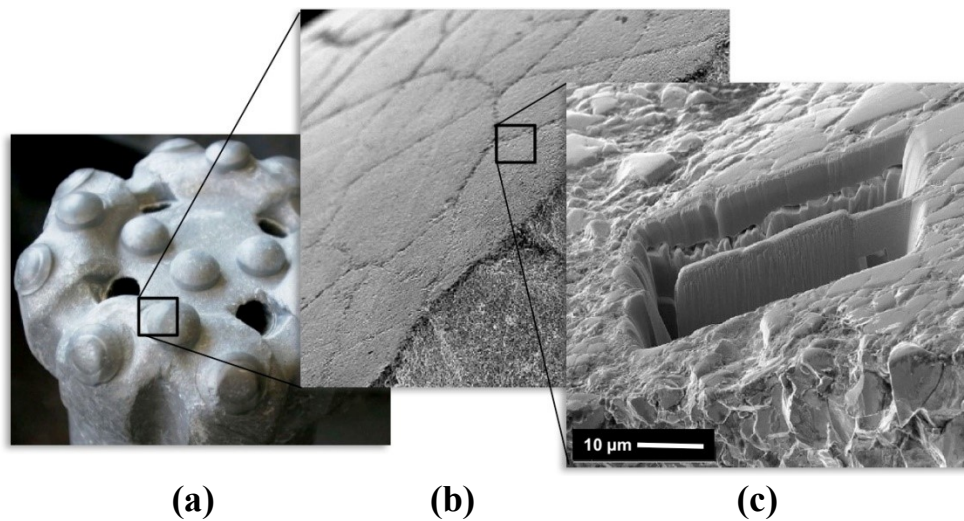


**Figure 19.** Appearance of a used percussion rock drill bit and the location of the studied cross-section. (a) The drill bit with its arrangement of attached CC drill buttons. (b) Close-up of one drill button, here with fracture cross-section to reveal modified surface layer (dark). (c) Detail showing the location of the TEM-sample prepared by the use of a FIB instrument.

Small buttons of CC are the active elements in crushing and fragmenting rock in percussive rock drills – see Fig. 19. Such buttons were sectioned using the FIB and studied by SEM and TEM. In conflict with the prevailing view that the temperature is too low to melt any rock material, a very thin layer of re-solidified rock material was found on top of the CC surface – see Fig. 20(a). TEM studies including energy dispersive X-ray spectroscopy (EDS) suggest that even below the outer surface, the

Co-matrix of the CC is gradually intermixed with rock material before it is removed – see figures 20 and 21. The rock mineral and the CC have formed a completely new composite material; a WC hard-phase kept together by an amorphous, Co-enriched binder phase of quartz. This tribofilm constitutes a unique form of cemented carbide, which to a large extent controls the wear rate of the button. Figure 21 shows the intimate, atomic level combination of the new matrix and the WC phase.

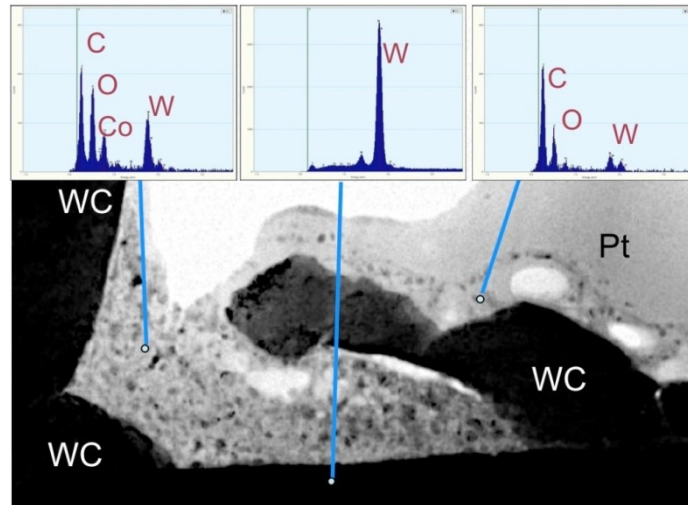


**Figure 20.** TEM micrograph and EDS spectra of indicated spots over a cross-section through the surface of a CC drill button used to drill in a quartz-containing rock mineral. The CC grain structure and a superficial layer of re-solidified rock material, including solidification pores can be distinguished. (Pt is used to protect the external surface during specimen preparation.)

## Conclusion

The surface layer of CC drill buttons transforms from the original WC/Co structure into a new composite. The intermixed layer is probably the modification which is most significant for the performance of the drill button. Here, the carbide phase is relatively intact while the binder consists of a mixture of cobalt and rock material. It should be expected that this composite exhibits properties significantly different from the original CC, due to the following alterations:

- a less ductile and possibly harder binder;
- probably an increased level of compressive stresses in the surface layer;
- probably wedge effects operating to widen cracks.

The rock penetration phenomena motivate special considerations in the development of new cemented carbide grades for rock drilling.

- Wear resistant CC materials should be designed to either obstruct intermixed layer formation or to generate such layers with high wear resistance.
- CC materials with improved fracture resistance should be developed to avoid rock material penetration.

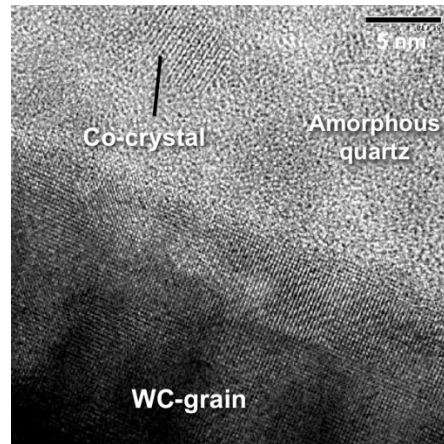


**Figure 21.** High-resolution TEM of the interface between a WC grain and an quartz rich tribofilm. An area of re-crystallized Co within the amorphous quartz is indicated. The WC-grain shows no indication of having been molten.

#### 4.8. Low-friction WS<sub>2</sub> film formed by selective transfer and chemical reactions

An example of positive tribofilm formation is obtained with a type of DLC coatings in boundary lubricated sliding against uncoated steel. Here, friction coefficients down to 0.05 have been recorded. In this specific example a film containing large amounts of WS<sub>2</sub> is continually formed on the uncoated steel surface, following a somewhat more complex route of formation. The DLC coating is of the WC/C type and the oil is a polyalphaolefin (PAO) additivated with compounds containing sulphur. A smooth nanocrystalline tribofilm is generated on the steel surface by chemical reactions between W extracted from the coating and S extracted from the additive compounds (see Fig. 22). Crystals of WS<sub>2</sub> were identified by X-ray photoelectron spectroscopy (XPS) and high-resolution TEM – see Fig. 23 [27].

Recently Stavlid et al. showed theoretically that alloying DLC coatings with Mo could also give low friction, due to formation of MoS<sub>2</sub> [24]. These films reduce the already low boundary lubricated friction by 40% or more. By including theory and extended experimental and surface analytical work, we are currently working to transfer these exciting lab results into industrially useful solutions.

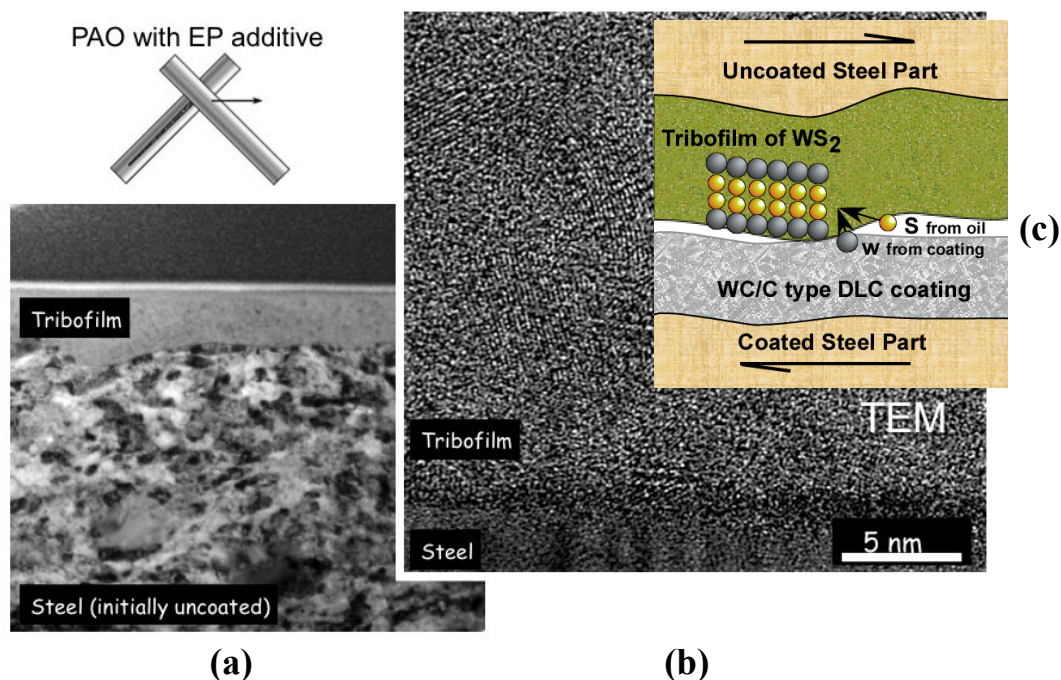


**Figure 22.** Cross-section of the tribofilm formed on a ball-bearing steel sample after rubbing against a W-doped DLC and (a) overview over the uncoated steel part after formation of the tribofilm, (b) HR-TEM of the tribofilm material, (c) simplified principle of the mechanism of formation [24].

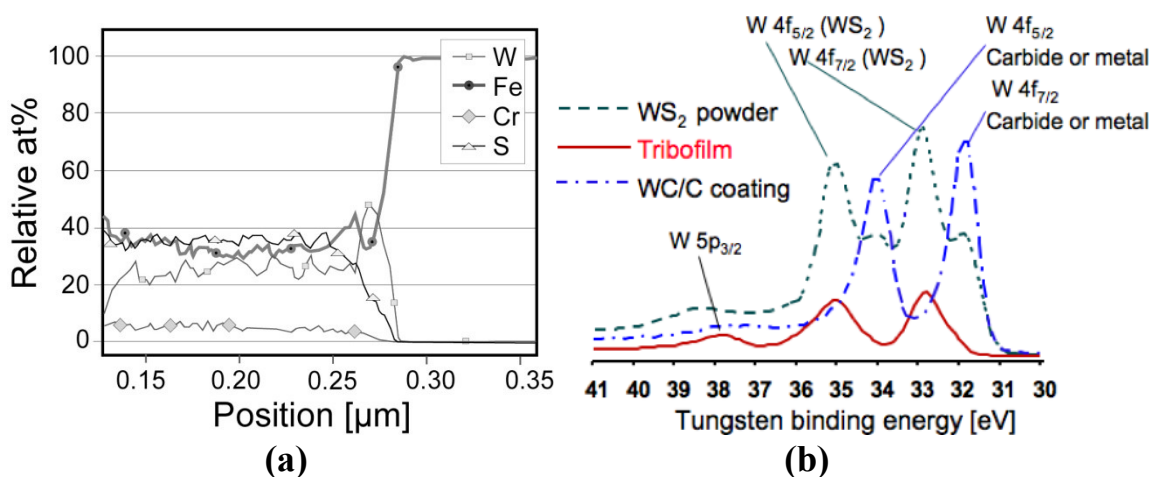


**Figure 23.** Chemical and depth profile analysis of the tribofilm in Fig. 22. (a) EDS elemental depth profile across the interface to the steel reveals high amounts of W, S and Fe in the film. (b) XPS spectrum comparing the composition of the tribofilm with the DLC coating (WC/C) and a reference  $WS_2$  powder [24, 27].

## Conclusion

A deposition type tribofilm forms on steel components in lubricated sliding against DLC coatings containing W or Mo. This film is formed by chemical reactions between wear products from both steel, DLC and sulphur containing additives in the lubricant. The film smoothens the contacting surfaces and reduces the friction considerably in boundary lubricated contacts.

## 5. Concluding remarks and key messages

As elucidated by the selected examples, tribofilms (using the broad definition of tribologically induced surface modifications) have decisive effects on the tribological performance of very different mechanical components and tools. It is *not* the original material that provides the wear resistance and friction level of the face seals, the brake pads, the cutting tools, the rock drill and so on. It is the tribofilms that constitute the real active surface layers of the different systems, and it is those films that will provide the properties to the components.

The list of examples could be made much longer, e.g. to include some of the very important and well investigated tribofilms formed by EP additives and friction modifiers in heavily loaded lubricated contacts, or by including the many forms of surface transformation of metals in sliding contact. Yet, the key messages would remain the same.

To meet the rapidly increasing tribological requirements of modern technology, we must extend our ability to optimize the use of tribofilms in the development of materials, coatings, surface finishing techniques and lubricants. This requires that we:

- Include analysis of tribofilms and surface modifications in all investigations of tribological performance and all evaluation of tribological tests. Their importance have often been highly underestimated. Researchers, mechanical designers and material developers have repeatedly been led to draw the wrong conclusions since their models of the tribological materials have been too simplistic.
- Appreciate the fact that the outermost, active part of the surface will invariably become modified, and hence systematically develop tribological materials and coatings that are tuned to achieve optimum properties after this modification.

## Acknowledgements

Our present and former Ph.D. students and colleagues Fredrik Svahn, Lars Hammerström, Nils Stavlid, Ernesto Coronel, Daniel Persson (now Maglione), Magnus Hanson, Ulrik Bestes, Adam Blomberg, Mikael Olsson, Johanna Olofsson, Jun Lu, Fredrik Lindberg and Stefano Rubino are gratefully acknowledged for offering their micrographs and results for the illustrations in this chapter.

## References

1. Hogmark, S., Jacobson, S., and Vingsbo, O. 1992. Surface damage. In *Friction, Lubrication and Wear Technology*, ASM Handbook 18, (Ed.: P. Blau), ASM International, pp. 176-183.
2. Blomberg, A. 1993. *Friction and wear of ceramics*. Uppsala University, Sweden.
3. Rigney, D.A., Fu, X.Y., Hammerberg, J.E., Holian, B.L., and Falk, M.L. 2003. *Scripta Mater.*, **49**, 977.
4. Rigney, D.A. 2000. *Wear*, **245**, 1.
5. Totten, G.E., and Fox-Rabinovich, G.S. (Ed.). 2007. *Self-Organisation During Friction*. CRC Press, USA.
6. Jacobson, S., and Hogmark, S. 2009. *Wear*, **266**, 370.
7. Coronel, E. *Solving Problems in Surface Engineering and Tribology by Means of Analytical Electron Microscopy*. 2005. Thesis No. 12, Uppsala University. ISSN: 1651-6214.
8. Hanson, M., Stavlid, N., Coronel, E., and Hogmark, S. 2007. *Wear*, **264**, 781.
9. Persson, D., Jacobson, S., and Hogmark, S. 2008. A physical model for the superior tribological performance of Stellites in highly loaded sliding contacts, *Wear*; in press.
10. Österle, W., Urban, I. 2006. *Tribology International*, **39**, 401.
11. Beste, U., Coronel, E., Jacobson, S. 2006. *Int. J. Refractory Met. Hard Mater.*, **24**, 168.
12. Berthier, Y. 1996, Maurice Godet's third body. In: Dowson, D., et al. (eds.), *The third body concept: interpretation of tribological phenomena*, Proc. 22nd Leeds-Lyon symposium on tribology, Elsevier, Amsterdam, The Netherlands.
13. Wood, R.J.K. 2007. *J. Phys. D: Appl. Phys.*, **40**, 5502.
14. Fischer, A., and Mischler, S. (Ed.) 2006, Tribocorrosion: fundamentals, materials and applications, *J. Phys. D: Appl. Phys.*, 39.
15. Olofsson, J., Jacobson, S., and Johansson, S. 2007. Analysis of the tribofilm formation on the friction drive surfaces of a piezoelectric motor. In *STLE/ASME Int. Joint Tribology Conf.*, San Diego, California, USA.
16. Olofsson, J., Lindberg, F., Johansson, S., and Jacobson, S. 2009. On the role of tribofilm formation on the alumina drive components of an ultrasonic motor. *Wear*, **267**, 1295.
17. Erickson, L.C., Blomberg, A., Hogmark S., and Bratthall, J. 1993. *Tribology International*, **26**, 83.
18. Ajayi, O.O., and Ludema, K.C. 1990. *Wear*, **140**, 191.
19. Adachi, K., and Kato, K. 2000. *Wear*, **245**, 84.
20. Andersson, P., and Blomberg, A. 1993. *Wear*, **170**, 191.
21. Blomberg, A., Hogmark, S., and Lu, J. 1993. *Tribology International*, **26**, 369.
22. Rainforth, W.M., 2004. *J. Mat. Science*, **39**, 6705.
23. Singer, I.S., Dvorak, S.D., Wahl, K.J., and Scharfb, T.W. 2003. *J. Vac. Sci. Technol. A*, **21**, 5.
24. Stavlid, N. 2006. On the formation of low-friction tribofilms in Me-DLC – Steel sliding contacts, Doctoral thesis, Uppsala University, Sweden.

25. André, B., and Jacobson, S. 2008. Comparisons between commercial low-friction coatings and emerging coating concepts in ball-on-disc tests – coefficient of friction, tribofilm formation and surface damage. In *NORDTRIB 2008*, Tampere, Finland.
26. Wilhelmsson, O., Rasander, M., Carlsson, M., Lewin, E., Sanyal, B., Wiklund, U., Eriksson, O., and Jansson, U. 2007. *Functional Materials*, **19**, 1611.
27. Podgornik, B., Hren, D., Vizintin, J., Jacobson, S., Stavlid, N., Hogmark, S. 2006. *Wear*, **261**, 32.
28. Lindqvist, M., and Wiklund, U. 2009. Tribofilm formation from TiC and nanocomposite TiAlC coatings, studied with Focused Ion Beam and Transmission Electron Microscopy. *Wear*, **266**, 988.
29. Lindquist, M. 2008, Self Lubrication on the Atomic Scale: Design, Synthesis and Evaluation of Coatings. Thesis No. 391, Uppsala University, Sweden. ISSN: 1651-6214.
30. Polcar, T., Evaristo, M., and Cavaleiro, A. 2007. *Vacuum*, **81**, 1439.
31. Bowden, F., and Hanwell, A.E. 1966. *Proc. Royal Soc. A*, **295**, 233.
32. Bowden, F., and Tabor, D. 1964. *The Friction and Lubrication of Solids. Part II*. Oxford University Press, Oxford, England.
33. Gardos, M.N. 1999. *Surf. Coat. Technol.*, **113**, 183.
34. Andersson, J., Duda, L., Schmitt, T., and Jacobson, S. 2008. *Tribology Letters*, **32**, 31.
35. Andersson, J., Erck, R.A., Erdemir, A. 2003. *Surf. Coat. Technol.*, **163–164**, 535.
36. Andersson, J. Microengineered CVD diamond surfaces – tribology and applications, 2004. Ph.D. thesis (Comprehensive summaries of Uppsala Dissertations from the Faculty of Science and Technology 977), Uppsala University, Sweden.
37. Martin, J.M., Grossiord G., Le Mognea, T., and Igarashi, J. 2000. *Wear*, **245**, 107.
38. Spikes, H. 2004. *Tribology Letters*, **17**, 469.
39. Hsu, S.M., and Gates, R.S. 2001. Boundary lubrication and boundary lubricating films. In *Modern Tribology Handbook* (Ed.: B. Bhushan), CRC Press, USA, pp. 455-492.
40. Callister Jr., W.D. (Ed.) 2003. *Materials Science and Engineering – An Introduction*. Wiley, USA.
41. Hogmark, S., Söderberg, S., and Vingsbo, O. 1979. Surface deformation and frictional heating of steel during machining and laboratory testing. *Proc. 3rd Int. Conf. on Mechanical Behaviour of Materials*, Cambridge, England, pp. 621-631.
42. Eklund, L.-H., and Hogmark, S. 1982. *Scand. J. Metall.*, **11**, 226.
43. Vingsbo, O., and Hogmark, S. 1981. Wear of steels. In *Fundamentals of Friction and Wear of Materials* (Ed.: D.A. Rigney), ASM: Ohio, USA, pp. 373–408.
44. Hogmark, S., Jacobson, S., and Coronel, E. 2007. *Tribologia* (Finnish Journal of Tribology), **26**, 3.
45. Persson, D. 2005. On the mechanisms behind the tribological performance of Stellites. Thesis No. 129, Uppsala University, Sweden. ISSN: 1651-6214.
46. Podgornik, B., Sandberg, O., and Hogmark, S. 2004. *Surface and Coatings Technology*, **184**, 338.
47. Schedin, E. Micro-mechanisms of sheet-tool contact during sheet metal forming, 1992. Ph.D. thesis, Royal Institute of Technology, Stockholm, Sweden.
48. Hogmark, S., Jacobson, S., and Wänstrand, O. 1999. A new universal test for tribological evaluation. In *Proc. 21st IRG-OECD Meeting* in Amsterdam, The Netherlands.
49. Hogmark, S., Olsson, M., and Blomberg, A. 1992. *Journal of Hard Materials*, **3**, 153.
50. Eriksson, M., and Jacobson, S. 2000. *Tribology International*, **33**, 817.
51. Eriksson, M. 2000. Friction and contact phenomena of disc brakes related to squeal. Comprehensive summaries of Uppsala Dissertations, Faculty of Science and Technology, Sweden, 537.
52. Eriksson, M., Lord, J., and Jacobson, S. 2001. *Wear*, **249**, 272.
53. Eriksson, M., Bergman, F., and Jacobson, S. 2002. *Wear*, **252**, 26.
54. Beste, U. 2004. On the nature of cemented carbide wear in rock drilling. Comprehensive summaries of Uppsala Dissertations, Faculty of Science and Technology, Sweden, 964.
55. Beste, U., and Jacobson, S. 2007. *Wear*, **264**, 1129.
56. Beste, U., Hogmark, S., and Jacobson, S. 2007. *Wear*, **264**, 1142.